REPORT DOCUMENTATION PAGE

AFOSR-TR-97 0129

1. AGENCY USE ONLY *(Leave blank)*	2. REPORT DATE	3. REPORT TYPE AND DATES COVERED
	May 2, 1997	FINAL REPORT 01 Jun 92 - 30 Nov 96

4. TITLE AND SUBTITLE
Impurity-Related Optical Emission
Alloys and Superlattices

5. FUNDING NUMBERS
61102F
2305/FS

6. AUTHOR(S)
Professor Dennis G. Hall

7. PERFORMING ORGANIZATION NAMES(S) AND ADDRESS(ES)
The Institute of Optics
University of Rochester
Rochester, NY 14627

8. PERFORMING ORGANIZATION REPORT NUMBER

9. SPONSORING / MONITORING AGENCY NAMES(S) AND ADDRESS(ES)
Air Force Office of Scientific Research
AFOSR/NE
110 Duncan Avenue, Suite B115
Bolling AFB, DC 20332-0001

10. SPONSORING / MONITORING AGENCY REPORT NUMBER
F49620-92-J-0336

11. SUPPLEMENTARY NOTES

a. DISTRIBUTION / AVAILABILITY STATEMENT
APPROVED FOR PUBLIC RELEASE: DISTRIBUTION UNLIMITED

12. DISTRIBUTION CODE

13. ABSTRACT *(Maximum 200 words)*

This report describes the results of experimental investigations of impurity-related, near-infrared optical emission from crystalline silicon and from silicon-germanium superlattices grown by molecular beam epitaxy (MBE). Radiative impurities can be introduced into silicon-germanium superlattices by post-growth ion implantation or by co-evaporation during growth. The research has demonstrated, using beryllium (Be) impurities, that radiative Be-pairs can be formed during MBE growth of silicon-germanium superlattices. Secondary-ion mass spectroscopy (SIMS) measurements reveal that the Be can be localized in the alloy layers of the superlattice. Investigations to date of superlattices (multi-quantum-wells) made up of alternating layers of silicon and a selected, Be-doped, silicon-germanium alloy show that quantum-confined bound-exciton emission can be observed when the alloy layers are below 5.0 nm in thickness. Spectral blue-shifts caused by quantum confinement have been observed. The results of theoretical calculations reveal that the isoelectronic bound-exciton emission from the Be-complex should be able to produce gain and laser action in a suitably defined, silicon-based, optical waveguide structure.

14. SUBJECT TERMS
Impurity-doped semiconductors;
optical emission from semiconductors.

15. NUMBER OF PAGES
27

16. PRICE CODE

17. SECURITY CLASSIFICATION OF REPORT	18. SECURITY CLASSIFICATION OF THIS PAGE	19. SECURITY CLASSIFICATION OF ABSTRACT	20. LIMITATION OF ABSTRACT
Unclassified	Unclassified	Unclassified	UL

Impurity-Related Optical Emission From Silicon, Silicon-Germanium Alloys and SiGe Superlattices

Final Report, May 2, 1997

Principal Investigator: Dennis G. Hall,
William F. May Professor and Director
The Institute of Optics, University of Rochester
Rochester, New York 14627
Telephone: 716-275-2134; FAX: 716-273-1072
e-mail: hall@moe.optics.rochester.edu

This program began on June 1, 1992. This report covers the period between June 1, 1992, and November 30, 1996 (the term of the program was increased by two no-cost extensions). It deserves mention that from the very beginning, the research involved the collaboration between two investigators, the named Principal Investigator and Dr. Joze Bevk of AT&T Bell Laboratories. Dr. Bevk is a recognized expert in the epitaxial growth of Group IV (silicon and germanium) thin films. Only the University of Rochester effort was funded by AFOSR. Dr. Bevk's portion of the collaboration was funded almost entirely by AT&T Bell Laboratories (now Lucent Technologies). His time and extensive growth and characterization facilities can be viewed as in-kind matching contributions that supplement the AFOSR funds. The close collaboration with a major industrial laboratory kept the University of Rochester research program very much at the forefront of the latest developments that might influence the research. Likewise, AT&T (now Lucent Technologies) was well positioned by the collaboration to make use of any output of the research that is important for device or system technologies. During the course of the research, additional collaborations developed with Prof. Irving P. Herman of the Department of Applied Physics at Columbia University and with Prof. Philippe Fauchet of the Department of Electrical Engineering at the University of Rochester.

I. Publications Citing AFOSR Support:

1. "Radiative Isoelectronic Complexes Introduced During the Growth of Si and $Si_{1-x}Ge_x$/Si Superlattices by Molecular Beam Epitaxy," Karen L. Moore, Oliver King, Dennis G. Hall, Joze Bevk, and Matthias Fursch, *Appl. Phys. Lett.* 65, 2705 (1994).

2. "Impurity-Related Photoluminescence from Silicon at Room Temperature," O. King and D. G. Hall, *Phys. Rev.* B15-I, 10661 (1994).

3. "Introduction of Radiative Isoelectronic Complexes During Molecular Beam Epitaxial Growth of Si and SiGe/Si Superlattices," K. L. Moore, O. King, D. G. Hall, J. Bevk, and M. Furtsch, (refereed) Proceedings of the Spring 1995 Meeting of the Materials Research Society, volume 378, pages 887 - 892, 1995.

4. "Use of Hydrostatic Pressure to Resolve Phonon Replica-like Features in the Photoluminescence Spectrum of Beryllium-Doped Silicon," S. Kim, I. P. Herman, K. L. Moore, D. G. Hall, and J. Bevk, Phys. Rev. B52, 16,309 (15 December, 1995-I).

5. "The Hydrostatic Pressure Dependence of Isoelectronic Bound Excitons in Beryllium-Doped Silicon," S. Kim, I. P. Herman, K. L. Moore, D. G. Hall, and J. Bevk, Phys. Rev. B53, 4434 (15 February 1996-II).

6. "A Si-based light-emitting diode with room-temperature electroluminescence at 1.1 eV," L. Tsybeskov, K. L. Moore, S. P. Duttagupta, K. D. Hirschman, D. G. Hall, and P. M. Fauchet, Appl. Phys. Lett. 69, 3411-3413 (1996).

7. "Intrinsic band-edge photoluminescence from silicon clusters at room temperature," L. Tsybeskov, K. L. Moore, D. G. Hall, and P. M. Fauchet, Phys. Rev. B54, Rapid Communications, R8361 (1996-II).

8. "Room-Temperature Photoluminescence And Electroluminescence From Er-Doped Silicon-Rich Silicon Oxide," L. Tsybeskov, K. L. Moore, K. D. Hirschman, S. P. Duttagupta, D. G. Hall, and P. M. Fauchet, Appl. Phys. Lett. 70, 1790 (1997).

9. "Isoelectronic Bound Exciton Photoluminescence in Strained Beryllium-Doped SiGe Epilayers and SiGe/Si Superlattices at Ambient and Elevated Hydrostatic Pressure," S. Kim, G. Chang, I. P. Herman, J. Bevk, K. L. Moore, and D. G. Hall, Phys. Rev. B55, 7130 (1997-I).

Additional manuscripts are in various stages of preparation, submission, or awaiting publication. Graduate student Karen Moore is writing her doctoral thesis as this report is being written.

Related Publications

1. "The Role of Silicon in Optoelectronics," (Invited Paper) Dennis G. Hall, Proceedings of the Materials Research Society, Volume 298, page 367, 1993.

2. "Radiative Isoelectronic Impurities in Silicon and in Silicon-Germanium Alloys and Superlattices," (by invitation) Thomas G. Brown and Dennis G. Hall, this chapter has been completed and will appear in an upcoming volume in the series *Semiconductors and Semimetals*, Academic Press, scheduled for publication in 1997.

II. Background

Silicon technology is clearly an all-important one in microelectronics. Its role in optoelectronics is less clear for at least two reasons. First, silicon's energy gap is indirect, which precludes efficient radiative recombination of electrons and holes. One cannot use band-to-band transitions in conventional, electronic-grade silicon as the basis for a light-source technology. Second, silicon has a centrosymmetric crystal structure, which means that silicon does not possess a linear electro-optic effect (Pockels' effect). Given those constraints, it is not clear how to use silicon technology to make high-performance light modulators and light sources. As discussed in my review paper [1], it is more apparent how to use silicon technology to fabricate such passive components as optical waveguides, grating filters, and the like.

This program of research was initiated to investigate one approach to the light-emission problem in silicon: impurity-related emission. The scientific community has several options open to it in it's attempts to overcome the limitations imposed by silicon's indirect bandgap. Among those are the use of superlattices to achieve improved performance via zone-folding, quantum

confinement to increase the radiative transition rate, and impurity-related emission. Porous silicon has received widespread attention; it is here considered to be a quantum-confinement effect. The challenge to identify a mechanism that will permit the efficient generation of light in a silicon-based materials technology is sufficiently great that it requires fundamental research in all areas. No single direction at this time can be said to be sufficiently promising to merit exclusive attention. One advantage to research in the Group IV materials is that it adds to the base of knowledge that supports the microelectronics industry. Fundamental research that connects with the silicon industry is a good idea on several counts.

One can distinguish two slightly different types of impurity-related mechanisms. The first is essentially an atomic transition in a semiconductor. The emission from erbium-doped silicon is the most visible current example. The second involves carrier trapping at an impurity. It is this second category that was of of primary (but not exclusive) interest at the beginning of the present research program. In particular, we explored the properties of the radiative decay of excitons bound to isoelectronic (also called isovalent) impurities in silicon, silicon-germanium alloys, and SiGe/Si superlattices. In this process, an electron or hole is trapped by the short-range potential of a neutral, isoelectronic complex. The Coulomb potential of the first carrier attracts the second, oppositely charged carrier to produce a bound electron-hole pair (a bound exciton). The electron and hole that make up the localized exciton eventually radiate, without the assistance of a phonon, to produce a photon. The radiative decay of excitons bound to isoelectronic impurities has already proved a commercially viable mechanism in light-emitting diodes made from the indirect III-V semiconductor GaP.

The silicon-germanium (Si-Ge) system is particularly attractive because of the possibility of fabricating layered structures. Any viable emitter technology will need not only an emission mechanism but also the ability to make waveguides, heterojunctions, quantum wells and superlattices. The SiGe system appears to be a good candidate to meet the structural needs of a device technology.

III. Objectives

The objectives of the research program were straightforward. The overall objective was to investigate the suitability of impurity-related mechanisms for efficient optical emission from Si, SiGe alloys, and SiGe/Si superlattices. In the process, we aimed to produce both ideas and experimental data that would improve the scientific understanding of radiative impurity complexes in those materials.

The research can be said to have had two principal parts: 1) a general investigation of impurity-related optical emission from silicon, and 2) an investigation of Be-related luminesence in SiGe alloys and SiGe/Si superlattices and quantum wells. A secondary component of the research took into consideration issues related to device structure that are naturally related to optical devices that might employ the mechanism of impurity-related optical emission. The two parts are intimately related. Much of the research centered on the properties of Be-related isoelectronic impurity complexes, the emission from which is among the brightest known in silicon. Taking the view that there remain many new radiative

isoelectronic impurity complexes yet to be discovered, we treat the radiative Be complex as a prototype complex. Exploring its properties in a variety of Si-related materials systems and structures helps us understand what to expect more generally from this category of impurities.

IV. Isoelectronic Bound Exciton Emission from Be-doped Silicon and Silicon-Germanium

Be atoms are known to form isoelectronic substitutional-interstitial pairs in silicon. The Be complex in Si binds an exciton that radiates efficiently into a sharp, no-phonon line at wavelength $\lambda = 1.149$ μm accompanied by a much weaker phonon replica near $\lambda = 1.23$ μm, as shown in Figure 1, below.

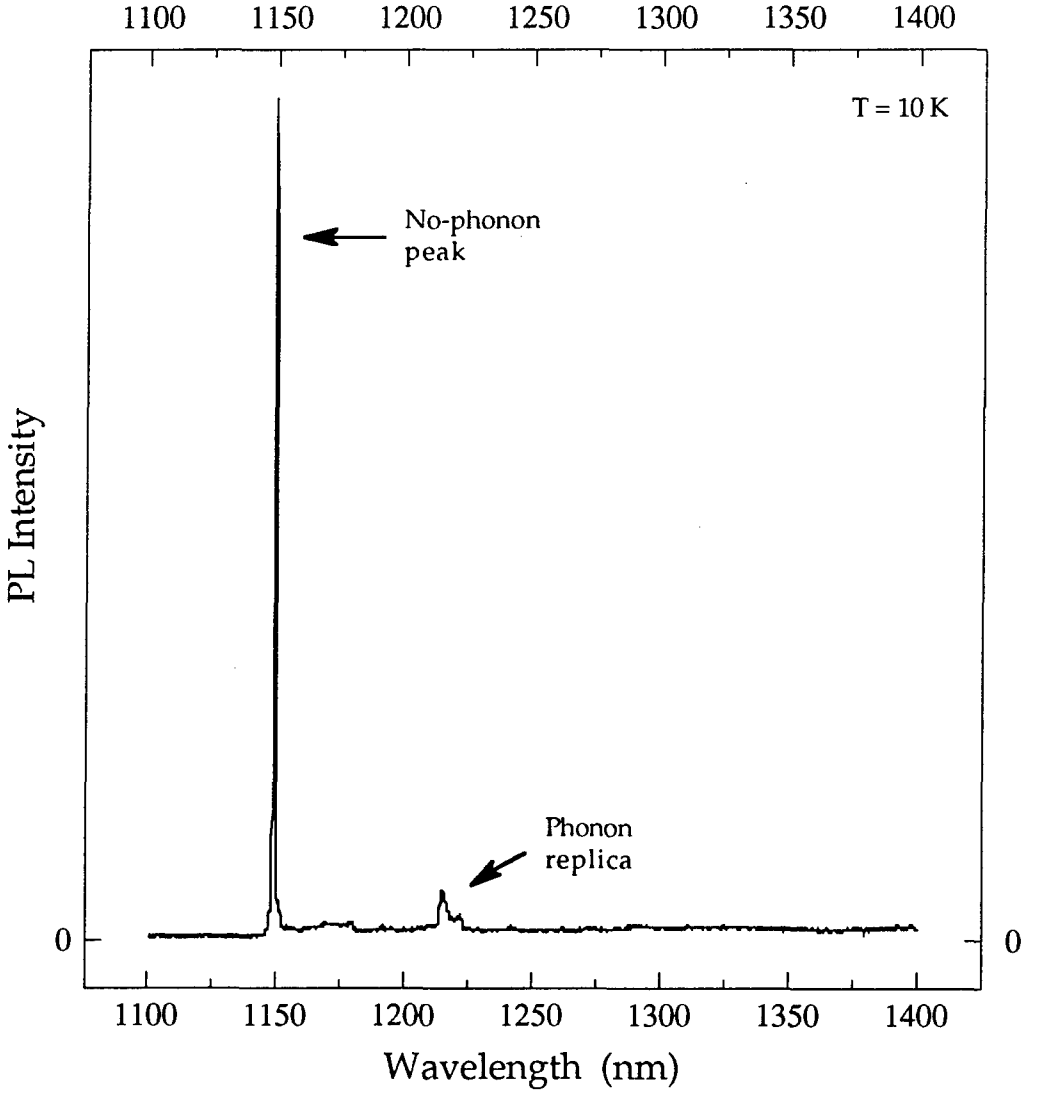

Figure 1. Measured photoluminescence intensity from Be-doped Si.

The external efficiency is approximately 1% at low temperatures, a surprisingly large efficiency. Near-infrared emission from the Be-related isoelectronic bound-exciton (IBE) is confined to low temperatures in silicon. Figure 2 shows the results of a typical measurement of the temperature dependence of the emission at wavelength $\lambda = 1.149$ μm. The emission persists only to approximately 50°K.

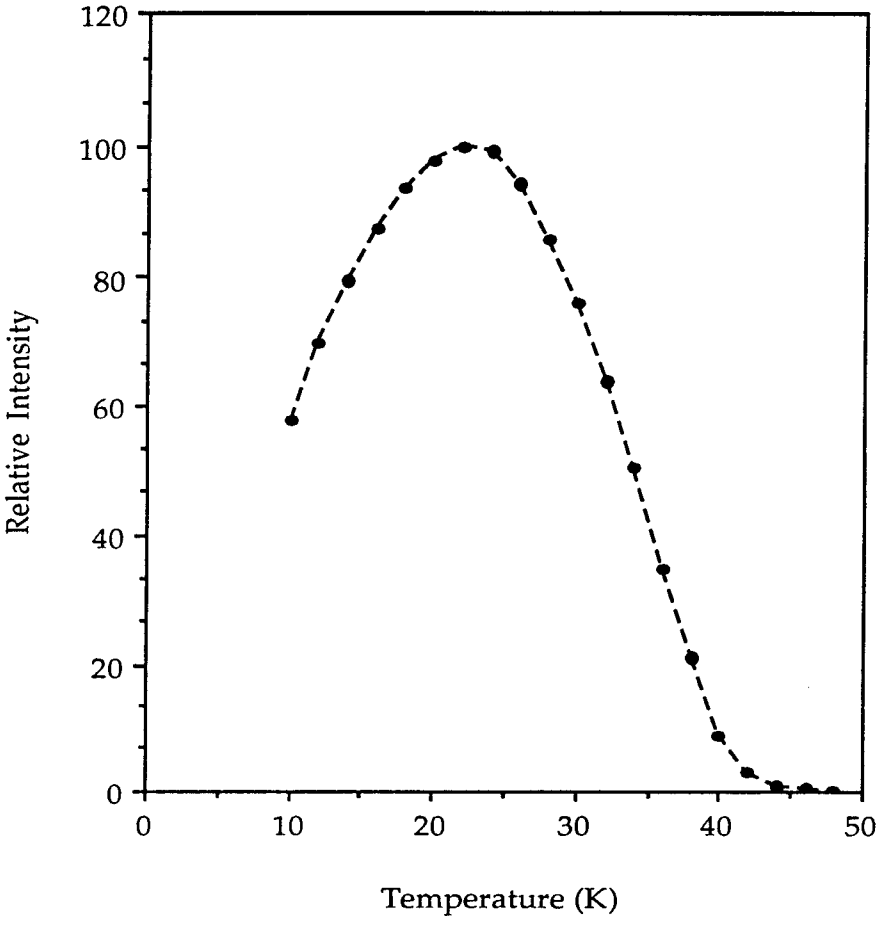

Figure 2. Temperature dependence of the emission from Si:Be measured at wavelength $\lambda = 1.149$ μm.

We have demonstrated that this Be prototype complex can also be formed in SiGe alloys grown by molecular-beam epitaxy (MBE). [2] Figure 3 (next page) shows the measured photoluminescence spectra from excitons bound to isoelectronic impurity complexes in several relatively thick, MBE-grown, Si-rich, $Si_{1-x}Ge_x$ alloy layers. The samples were grown by Dr. Joze Bevk at Bell Laboratories as part of the aforementioned collaboration. Typical layer thicknesses exceeded 100 nm. Spectra are shown for Ge fractions ranging from $x = 0$ (pure silicon) through $x = 0.20$. The upper spectrum is the same as that presented in Figure 1. The no-phonon line shows a steady shift to longer wavelengths (lower energies) with increasing x, reflecting the decrease in the energy gap with increasing x. In the samples used for Figure 3, Be was introduced by post-growth ion implantation. [2]

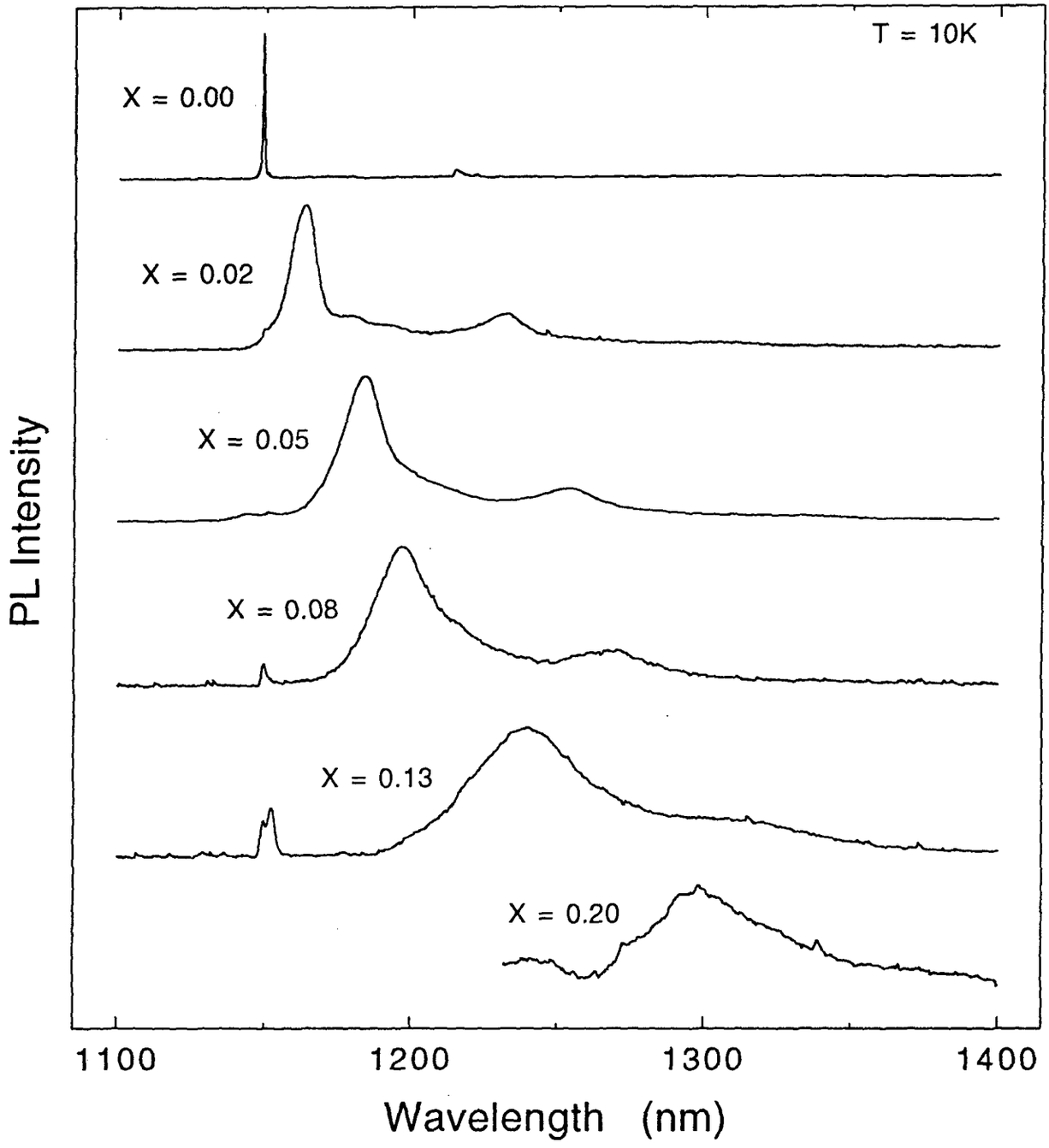

Figure 3. Photoluminescence intensity as a function of wavelength for Be-doped SiGe alloys. x designates the fraction of Ge in the alloy.

We have also demonstrated that the Be complex can be formed in other layered structures, including epitaxial Si layers grown onto heavily doped silicon substrates [3] and SiGe/Si superlattices grown on Si. [4] The former was carried out in collaboration with Dr. Richard Soref of the U.S. Air Force Rome Laboratories (Hanscom AFB), and demonstrated the impurity luminescence, observed in edge emission, would excite the waveguide modes supported by the epitaxial-Si layer. In all cases, the impurities were introduced by ion implantation, a convenient technique that also has its drawbacks, particularly the possibility ion implantation might cause crystal damage, producing defects. Introducing the prototype Be complex during growth, if possible, would be a preferable option.

V. Introduction of Be Impurities During MBE Growth: PL Data

As part of the collaboration with Bell Laboratories, the MBE growth chamber was modified to enable Be impurities to be introduced into Group IV samples during growth. The principal modifications were:

1. Addition to the system of a Be effusion cell;
2. Design and installation of a shuttering system for automated depostion of of superlattice structures;
3. Modification of all e-gun sources to reduce the level of background impurities;
4. Design and installation of a water-cooled shielding system to minimize the cross-contamination from other dopant sources (especially Sb) in the MBE system.

AFOSR funds were used to purchase a few items connected with the upgrade of the MBE system for this research:

1. A wafer-manipulator heater assembly;
2. Two In-free moly wafer holders dedicated to Be-doped structures;
3. A power supply for the Be effusion cell.

Although a number of unexpected difficulties arose during the MBE system modification (leaks, mechanical failures, and a problem with a new, but contaminated valve that had to be returned and replaced), everything was eventually brought under control.

Creating the desired radiative Be complex during growth requires introducing the Be in such a way that substitutional-interstitial pairs are formed. This proved relatively straightforward. Figure 4 (see next page) shows a plot of the measured photoluminescence (PL) intensity from four early, MBE-grown *silicon* epitaxial layers doped with Be during MBE growth in Dr. Bevk's chamber at AT&T. Each sample was grown with a different Be-cell temperature. The PL was measured at temperature T = 10K at wavelength λ = 1.149 μm. The appearance of that signal means that the Be was incorporated and that Be pairs were formed. One can see from the data that an order of magnitude change in the resultant PL intensity

Figure 4. Calibration plot for epitaxial silicon layers doped with grown-in Be.

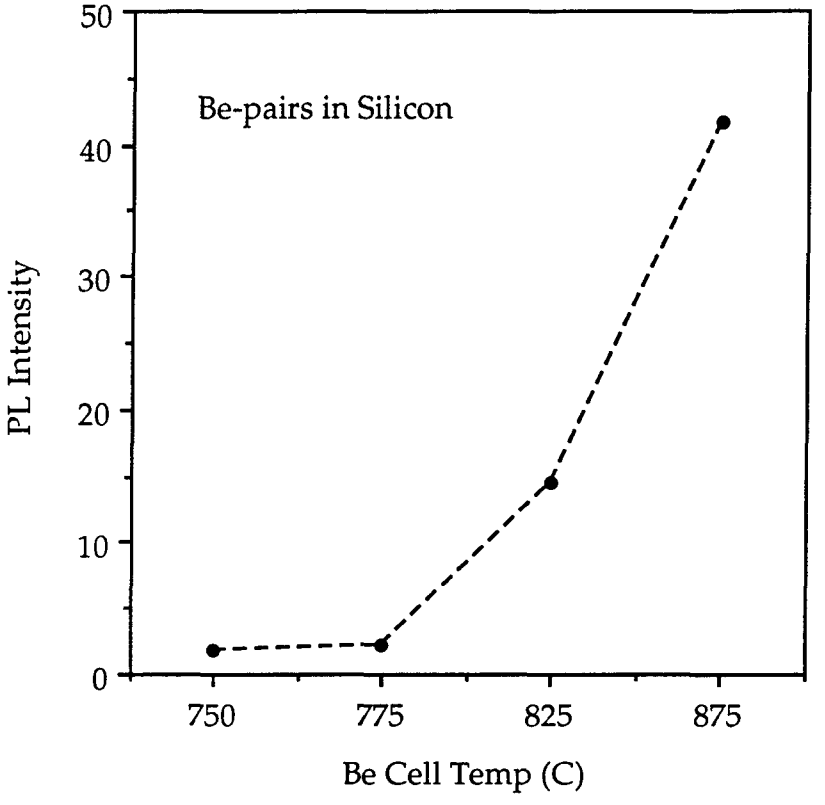

accompanied an increase in the Be-cell temperature by 125C. The PL spectra obtained from all samples was identical to that presented in Figure 1.

Silicon that is ion-implanted with Be usually requires a post-annealing step (10 minutes at T = 590°C) to activate strong luminescence. The samples with grown-in Be did not require annealing, so it appears that the required Be pairs formed during Si growth, a point of critical importance for obtaining luminescent centers. For the sample grown at Be-cell temperature 775°C, SIMS (secondary-ion mass spectrometry) analysis revealed a Be concentration of approximately 7×10^{17} cm^{-3} in the MBE-grown layer, showing appreciable concentrations can be achieved.

Turning to the SiGe system, our investigations revealed that the radiative Be complexes could also be incorporated into SiGe/Si superlattices. To facilitate comparisons with the results of our previous work on ion-implanted superlattices, we grew and examined superlattices composed of ten periods, with each period made up of a 50 Å thick layer of $Si_{0.92}Ge_{0.08}$ and a 100Å thick layer of Si. The alloy layers were grown at a temperature T ~ 450°C, and the shutter in front of the Be source, held at temperature $T = T_{Be}$, was opened during growth of the central 17 Å of each alloy layer. The first 20 Å of each Si layer was grown at temperature T ~ 300°C, after which the growth temperature was raised to T ~ 550°C to complete the Si layer growth. As with the Si samples described earlier, the Be-related IBE emission was observed without the need for post-growth annealing, which means that the required Be pairs formed during growth of the SiGe alloy.

Figure 5 shows on an expanded scale a comparison of the measured photoluminescence spectra for two $Si_{0.92}Ge_{0.08}$ /Si (50 Å/100 Å layer thicknesses) superlattices.

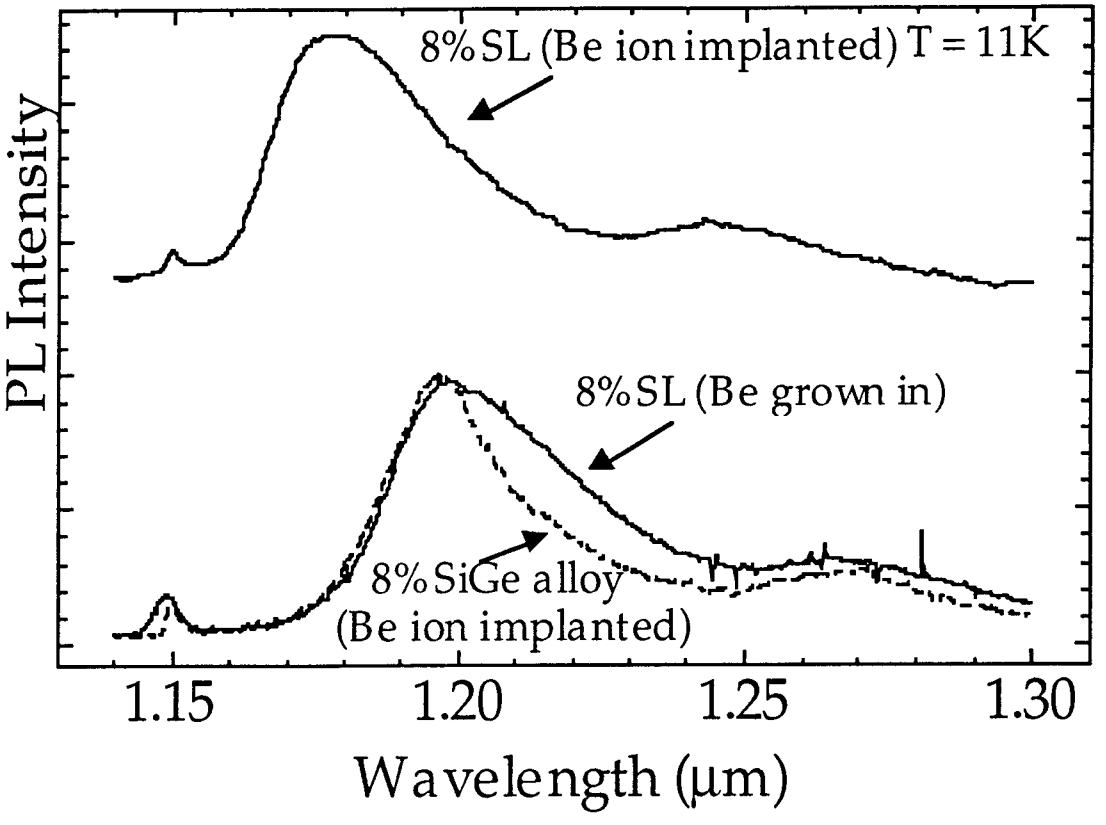

Figure 5. PL spectra for SiGe:Be (SL designates superlattice). Each SL contains 50 Å thick (8%) alloy layers alternating with 100 Å thick silicon layers.

The upper curve is the same as that we measured earlier for a Be-implanted superlattice. The lower curve is that for a superlattice with grown-in Be. In both cases, the small feature near wavelength λ= 1.15 μm is due to emission from excitons bound to Be that has found its way into the Si substrate. As we reported earlier in connection with ion-implanted samples, the position of the Be IBE no-phonon intensity peak for the superlattice is blue-shifted from that for a thick alloy layer. This can be understood as arising from the fact that ion implantation introduces Be not only throughout the alloys layers, but also throughout the Si layers of the superlattice. A theoretical model shows that the exciton binding energy varies with the position in the superlattice of the Be-pair to which the exciton is bound. Because the Be distribution is smeared out in the superlattice, the no-phonon line is shifted and the linewidth is broadened in a predictable way.

One of the stated advantages of introducing the Be impurities during growth is the ability to control the location of the Be atoms to a degree that cannot be achieved with ion implantation. Our efforts to control the position of the Be atoms by opening the shutter in front of the Be cell only during growth of the central 17 Å

of each alloy layer were successful. The lower curve in Figure 5 shows that the Be-related no-phonon emission line is located at the same wavelength as that from a thick alloy layer implanted with Be. The line remains broader than that from a Be-implanted thick-alloy layer (several thousand Å), but the absence of the aforementioned blue-shift argues strongly that the Be has been confined reasonably well in the alloy layers of the superlattice. The observation in Figure 5 that the no-phonon line from the superlattice with grown-in Be occurs at the same wavelength as that from a thick alloy of the same composition confirms our earlier prediction. That the linewidth has not decreased to that of the implanted alloy suggests other factors are at work in the grown-in samples, as will be briefly discussed shortly.

Further evidence that the Be is localized in the alloy layers can be found from a SIMS analysis. Figure 6 shows the results of a SIMS measurement of the Be concentration for a sample grown with T_{Be} ~ 800°C, the same sample used to obtain the lower curve in Figure 5.

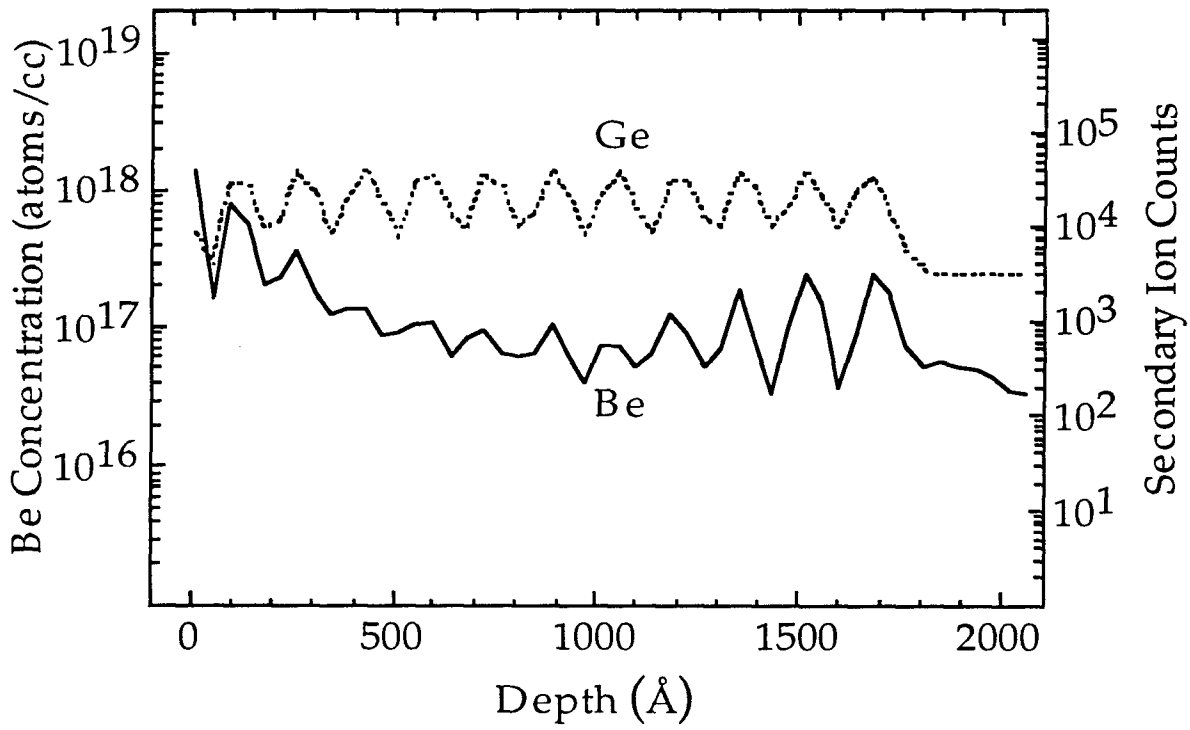

Figure 6. Results of SIMS measurements.

Note that the concentrations labeled on the left vertical axis of the plot apply only to the curve for Be. The Ge lines are present only to indicate the locations of the alloy and Si layers. Several things are evident from Figure 6. First, the Be concentration oscillates with depth and tracks the Ge signal, indicating the Be atoms are more highly concentrated in the alloy layers than in the Si barrier layers. Second, given that the alloy layers are only 50 Å thick, and that we attempted to introduce Be into only the central region of each alloy layer, the limited depth resolution of the SIMS technique produces some degree of averaging in Figure 6. Given this averaging, we

estimate the peak Be concentrations to exceed a few times 10^{17} cm^{-3}, in agreement with the measured integrated Be dose per SiGe layer of $6 - 10 \times 10^{10}$ cm^{-2}. Third, the fact that the deepest alloy layer, the first one grown, shows the highest Be concentration most likely means that the Be charge in the effusion cell had not yet cooled completely from earlier outgassing. Be sublimes rather than evaporates from the liquid phase, resulting in poor thermal contact between the solid Be charge and the effusion cell. In later growths, more time was allowed for the Be cell to cool to the desired temperature prior to starting deposition.

The Be concentration in the alloy layers depends on the Be cell temperature. The concentration achieved in the sample associated with Figures 5 (lower curve) and 6 produced a healthy, easily detected Be IBE no-phonon line. Increasing the Be cell temperature does not necessarily increase the PL intensity, however. A SIMS analysis of a second superlattice for which the Be cell temperature was increased to $T_{Be} \sim 905°C$ shows many of the same features as that in Figure 6, but with the significant difference that the Be concentrations in the alloy layers are more than two orders of magnitude higher than those shown in Figure 6. Our growth technique clearly makes it possible to control the Be concentration over a rather wide range. Interestingly, the sample grown with the higher Be-cell temperature ($T_{Be} \sim 905°C$) exhibited no characteristic SiGe:Be-related IBE PL-emission lines. A third superlattice grown using an intermediate Be-cell temperature did produce the characteristic Be-related luminescence.

Since the solid solubility of Be in Si is reported in standard references to be "negligible," it is almost certain that the very high Be concentration ($> 10^{20}$ cm^{-3}) in the sample grown at $T_{Be} = 905°C$ substantially exceeds the Be solid solubility in the alloy. The absence of the SiGe:Be-related PL from that sample indicates some form of concentration quenching or a possible breakdown of pseudomorphicity with a large attendant defect density. The issue is complicated by the fact that it is Be pairs that bind the exciton; the Be concentration provided by the SIMS measurement is not sufficient to determine the number or density of Be pairs. There is preliminary evidence that the width of the no-phonon line increases with the Be concentration, which suggests that the unexpectedly large linewidth associated with the unshifted (with respect to the thick alloy line) no-phonon line in the lower curve in Figure 5 might reflect the presence of a substantial density of unpaired or clustered Be atoms. Further, as mentioned earlier, the data described here were obtained using as-grown superlattices with no post-growth annealing. Annealing might well be required for the higher Be concentrations, just as it is needed for Be-implanted Si. Indeed, different alloy compositions might require different types of post-growth processing to achieve the greatest density of Be pairs.

To provide an intermediate summary, we have thus far shown that radiative isoelectronic bound-exciton complexes can be formed during MBE growth of Si and Si-rich SiGe/Si superlattices. Be-cell temperatures in the 800 - 900°C range along with growth temperatures in the 450 – 600°C range are adequate to produce Be concentrations in excess of 10^{17} cm^{-3}. Because the radiating exciton is bound to an isoelectronic Be pair, observation of the IBE no-phonon line is clear evidence that

Be pairs form during sample growth. The previously observed blue-shift of the no-phonon line from a Be-implanted SiGe/Si superlattice is absent for superlattices with Be grown directly into the alloy layers, confirming an earlier theoretical prediction.

VI. Optical Emission from Be-doped SiGe/Si Quantum Wells

After establishing we could introduce radiative impurity complexes into MBE-grown SiGe layers with a reasonable degree of spatial selectivity, we turned our attention to a search for direct evidence of quantum confinement effects using samples similar to those described in the last section, and illustrated here for clarity below. Figure 7 shows a few layers of a Be-doped SiGe/Si superlattice.

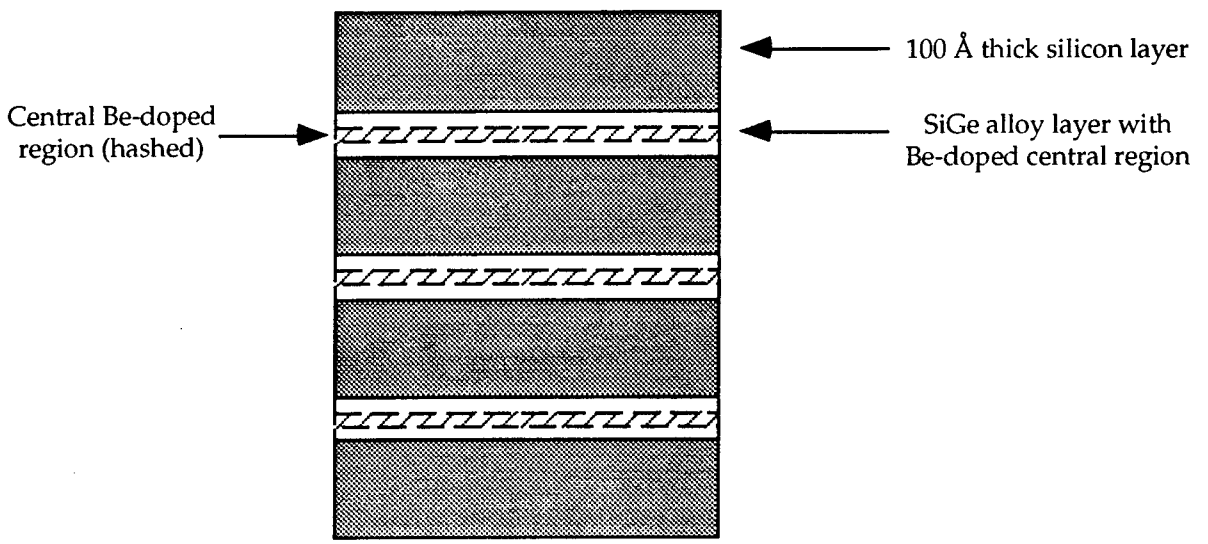

Figure 7. Be-doped SiGe/Si superlattice.

In Section V, we presented SIMS data to show that we had managed to concentrate the light-emitting Be impurities in the central 1.7 nm of 5.0-nm-thick $Si_{0.92}Ge_{0.08}$ "quantum wells" (the sample had ten periods with the structure shown in Figure 7; the sketch shows only three periods for illustration). We also presented photoluminescence (PL) data that showed that the PL spectrum from the excitons bound to the Be pairs was virtually identical to that from Be introduced into a thick (bulk) sample of the same alloy composition. Therefore, while we succeeded in controlling the location of the radiating impurities, the combination of the 5.0 nm alloy-layer thickness and the relatively small Ge content of the alloy was insufficient to provide quantum confinement. Still, it was an important intermediate step toward that goal.

To see the importance of controlling the placement of radiative isoelectronic impurities in a quantum-well sample, consider the data presented in Figure 8 (see next page). The open squares represent the results of measurements for thick alloy samples that were implanted with Be. The solid circle labeled SL50I was obtained from a superlattice sample with the same basic structure as in Figure 7, with x = 0.08,

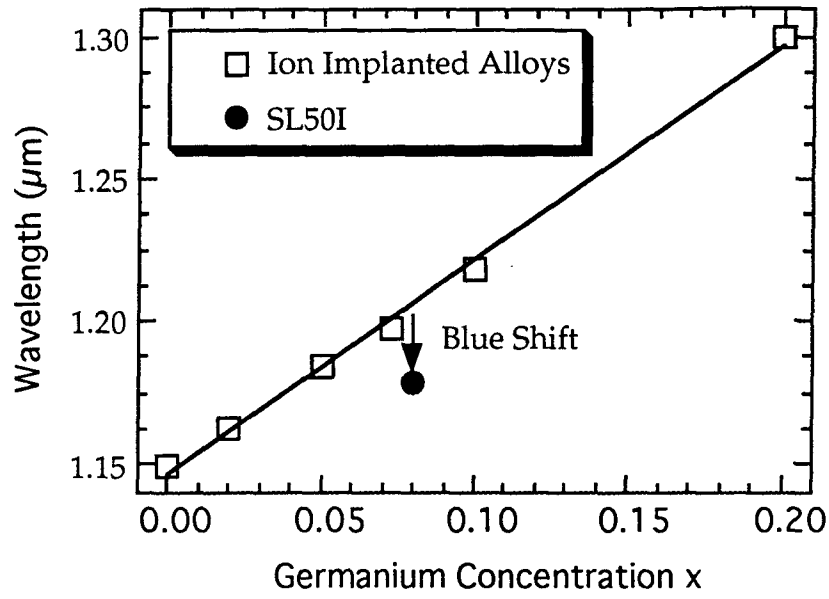

Figure 8. Measured wavelength of the bound-exciton (no-phonon) emission peak from several $Si_{1-x}Ge_x$ samples at T = 11K.

alloy-layer thickness of 5.0 nm, but with implanted instead of grown-in Be. The apparent blue-shift is not evidence of quantum confinement because of the effects associated with the extended spatial distribution of the implanted Be centers, as mentioned earlier. The exciton binding energy is position-dependent; a detailed analysis of the effects of this extended Be distribution is to produce a blue-shift, as explained in our November 1994 paper in *Applied Physics Letters* (paper #1 on the list in Section I; see page 1 of this report). When the Be is concentrated in the centers of the alloy layers by introducing it during growth, the above blue-shift disappears.

To search for true quantum-confinement effects requires either thinner alloy layers or alloy layers with greater Ge content, or a combination thereof. We were able to observe true quantum confinement by reducing the alloy-layer thickness from 5.0 nm to 2.0 nm while holding the Ge content of the alloy layers fixed at the earlier value x = 0.08. (Refer again to the basic sample structure illustrated in Figure 7.) Figure 9 (see next page) shows on an expanded scale the measured PL spectra for several samples. Samples SL20 (alloy-layer thickness = 2.0 nm) and SL50 (alloy-layer thickness = 5.0 nm) both contained Be that had been introduced during MBE growth; x = 0.08 for both samples. As mentioned earlier, sample SL50 contains alloy layers that are too thick to produce quantum-confinement effects in the bound-exciton spectrum, as evidenced by the fact that the SL50 PL spectrum is nearly the same as that from Be implanted into a thick, MBE-grown alloy layer with the same composition (x = 0.08). However, sample SL20 shows a significant blue-shift, from wavelength $\lambda = 1.20\ \mu m$ to $\lambda \sim 1.16\ \mu m$, demonstrating that the reduced alloy-layer thickness has brought us into the quantum-confinement regime. The interfaces are

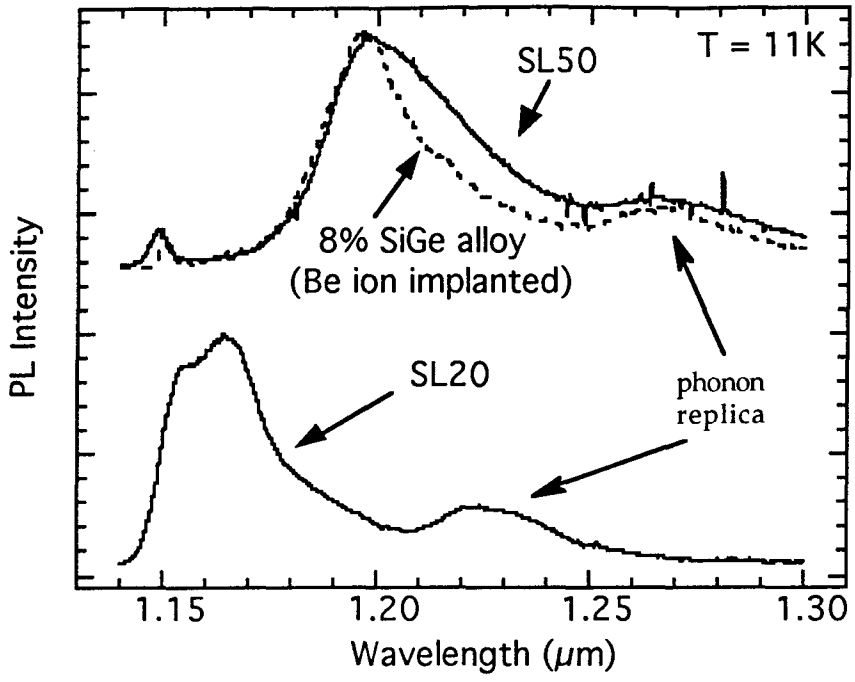

Figure 9. Measured PL spectra. Sample SL20 (SL50) has an alloy-layer thickness of 2.0 nm (5.0 nm). The dashed curve if for a thick alloy ion-implanted with Be.

now intruding on the bound-exciton wavefunction sufficiently to modify the emission spectrum.

Figure 10 shows the SIMS data for sample SL20, demonstrating that the

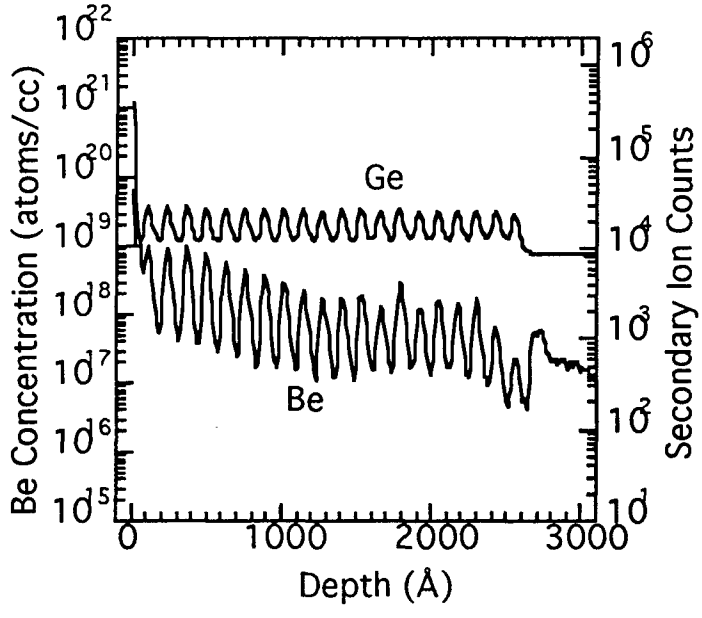

Figure 10. Be concentration vs. depth in superlattice SL20. The composition of SL20 is given in the text (see Figure 7).

grown-in Be follows quite well the Ge concentration that marks the locations of the alloy layers in the superlattice sample. Note: the concentration numbers on the vertical axis indicate only the Be concentration, not that for Ge. Also, the SIMS resolution is insufficient to allow the measured Be-concentration to fall completely to zero in the 10-nm-thick Si barrier layers. The same is true for the Ge signal.

Figure 11 shows the PL spectrum from another sample with the same basic structure shown in Figure 7, but with alloy layers of thickness 2.0 nm and increased Ge content x = 0.13. In Figure 11 that spectrum is compared with the PL spectrum from a thick Be-doped alloy (0.3 μm). A blue shift of the no-phonon line is again

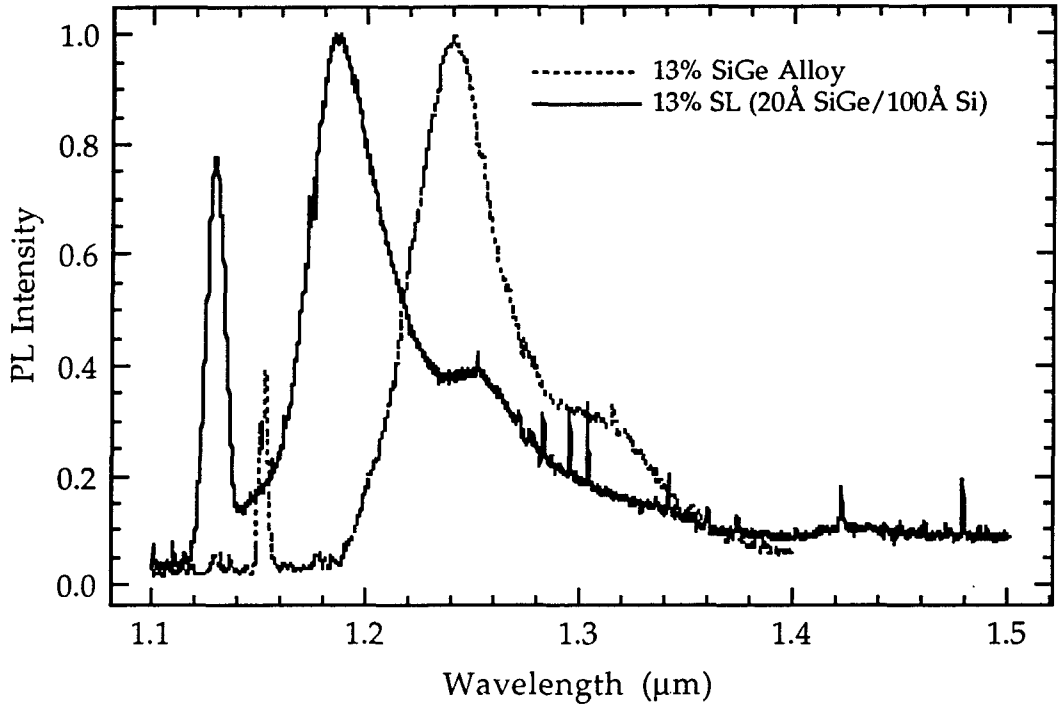

Figure 11. Comparison of the Be-related bound-exciton emission from a superlattice and a "bulk" alloy for x = 0.13.

apparent, this time from wavelength λ = 1.24 μm to approximately λ = 1.18 μm. The shoulders on the long-wavelength side of both peaks are the characteristic phonon replicas. The sharp peak near λ = 1.15 μm for the "thick" alloy layer arises from Be that has found its way into the silicon substrate as a result of the Be-implant. The bound-exciton no-phonon line for Si:Be occurs at precisely that wavelength. This is absent in the other spectrum, of course, because Be was grown in under controlled conditions, not implanted, so there was less opportunity for the Be to migrate into the substrate. The sharp peak in the PL spectrum for the superlattice (SL) sample (solid curve) is very likely produced by the phonon-assisted (band-edge) free exciton in the silicon substrate. Its absence in the alloy sample is probably due to absorption in the relatively thick alloy overlayer. The superlattice in this case contains relatively little alloy: only ten periods were grown, producing a total alloy thickness of 20 nm, much less than the 300 nm thickness of the alloy in the other sample. Again, the data in Figures 9 and 11 suggest that we have indeed reached the regime

where the excitons bound to the Be isoelectronic pairs experience quantum confinement, an important result.

As quantum-confinement effects set in, one hopes to see improvements in the temperature dependence of the luminescence. Indeed, one motivation for the present work was to investigate whether or not quantum confinement in the SiGe/Si system is an effective means for improving the PL-vs.-temperature signature shown in Figure 2 for Si:Be. To date, bound-exciton emission from isoelectronic impurities in Si has not been observed above perhaps (generously) T = 200C, something achieved using the sulfur-related impurity system we discovered in the middle 1980s. [5,6] However, we have not been able, so far, to find a way to activate the sulfur-related complex in SiGe alloys, which makes it difficult to investigate quantum-confined bound excitons in SiGe/Si doped with sulfur. However, since we did succeed in forming the isoelectronic Be complex in SiGe alloys, the Be complex was the natural one to use to investigate quantum confinement.

Figure 12 shows the measured temperature dependence of the PL measured from three samples: the superlattice with grown-in Be, for which the spectrum is shown in Fig. 11 (sample JB-212C, dark circles), a Be-implanted "thick" alloy layer (open circles), and Be-implanted silicon (open squares). The Ge content was x = 0.13 for all $Si_{1-x}Ge_x$ alloy layers used for the plots in Fig. 12. As can be seen from the

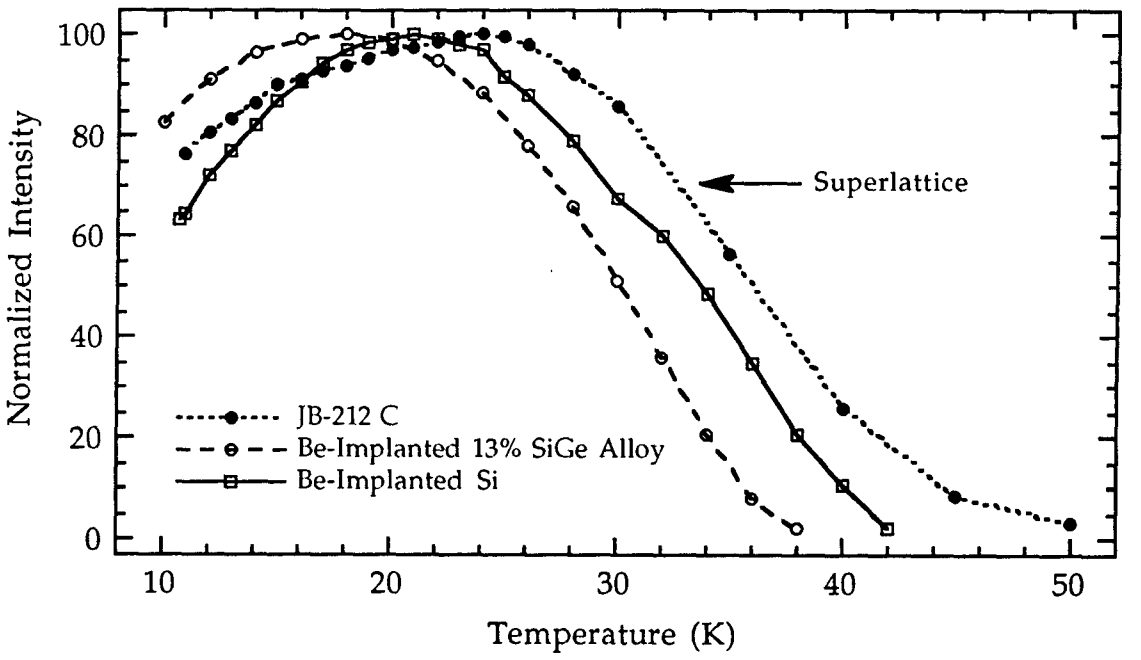

Figure 12. Measured dependence of the intensity of the no-phonon emission line from the Be-related bound-exciton in three hosts.

Si:Be data, the Si:Be system is intrinsically a low-temperature system with peak luminescence occurring near T = 20K. The external efficiency of the Si:Be bound-exciton emission is respectably high (~1%) at T = 20K, but the luminescence crashes at too low a temperature to be of commercial importance at this point. The data in

Figure 12 offers some encouragement, however, because of the improved behavior that accompanies the use of the SiGe quantum wells. It remains to be seen if this improvement will continue with a further decrease in the alloy-layer thickness and an increase in the Ge content of the alloy, but the present results are moderately encouraging.

VII. Room-Temperature Optical Emission from Silicon

This work is motivated by the desire to examine the behavior of a luminescent center in silicon that, unlike the Si:Be or the SiGe:Be bound-exciton emission, persists to room temperature. We have previously discovered and reported sulfur-, selenium-, and tellurium-related impurity centers in silicon. We present here the results for what appears to be another chalcogen-related system in Czochralski (CZ)-grown silicon. The PL signal from this system exhibits two distinct bands whose relative intensities vary with temperature. This system is remarkable, however, in that the high temperature band has a significant PL signal strength which persists to room temperature. Reports in the literature of room temperature luminescence in silicon are rare. While phonon-assisted free carrier combination is observed in Si, the efficiency of this process is understandably low, with a measured internal quantum efficiency (QE) of $10^{-4} - 10^{-6}$. Recently, band-edge recombination at room temperature in a SiGe/Si quantum well structure has also been reported to have an electroluminescent internal QE of 2×10^{-4}. Spectra have been shown for room temperature luminescence from Er-doped silicon, but we know of no literature reports of the quantum efficiency to date.

Figure 13 (see next page) shows PL spectra for temperatures T = 30K, 130K, and 300K for a typical sample which, in this case, consisted of a portion of a <100> oriented, p-type (resistivity = 40 Ω-cm) CZ Si wafer manufactured by Monsanto. The sample was prepared for this experiment by heating it in air at T = 450°C for 72 hours. The PL spectra were obtained with the sample mounted in an Air Products closed-cycle He cryostat and excited with the 676 nm line of a Kr^+ ion laser. The resulting PL signal was chopped at 100 Hz, dispersed using a McPherson 0.35 meter grating monochromator, and detected using a North Coast liquid-nitrogen cooled Ge detector and a Stanford Research Systems lock-in amplifier.

As in the case of our previously observed chalcogen impurity centers, the spectrum contains two distinct components. The peak near wavelength $\lambda = 1.6$ μm (energy = 0.767 eV) in the T = 30K spectrum is the well-known P-line. As the sample temperature is raised, we find that the P-line broadens somewhat while a new, much broader emission band rises from the background. These two components are clearly evident in the T = 130K spectrum. At yet higher temperatures, the P-line diminishes with respect to the broad band such that, at room temperature (T = 300K), only this band is evident. The apparent shift to higher energies (shorter wavelengths) of the emission peak as the sample temperature is raised from T = 130K to T = 300K is actually an artifact introduced by the declining sensitivity of the Ge detector for $\lambda > 1.6$ μm. To show this is indeed the case, we measured the PL

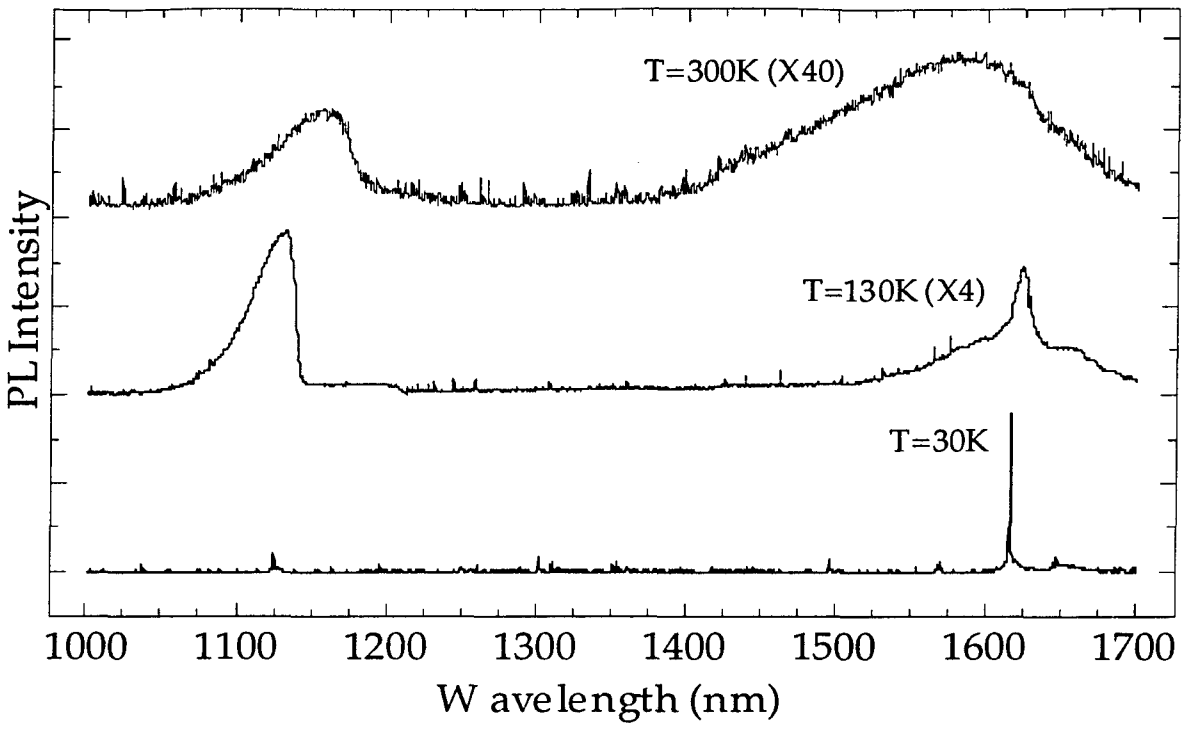

Figure 13. Spectrum from annealed silicon at three temperatures.

spectrum at T = 300K for the same sample using a Judson Infrared liquid-nitrogen-cooled InAs detector. The result appears in Figure 14. This detector is noisier and less sensitive than the Ge detector, but its spectral response is nearly flat over the spectral extent of the broad peak. The room-temperature PL clearly peaks near λ = 1.7 μm, demonstrating that the above-mentioned shift to shorter wavelengths is indeed a detector artifact. Another interesting feature of the higher temperature spectra in Figure 13 is the presence of a strong PL component near the band-edge. We find that for this sample at T = 300K, this band is enhanced by about two orders of magnitude over that of an unannealed control sample from the same wafer.

Note that while we present spectra for a single sample in Figure 13, we have observed identical features (with varying intensities) from a large number of commercial CZ-grown Si samples, regardless of conductivity, type, or orientation. We do not, however, observe either the enhanced band-edge emission or the longer wavelength PL component from magnetic-CZ-grown or float-zone refined wafers, or from layers grown by a number of epitaxial techniques. This strongly suggests that the luminescence results from a defect complex in which oxygen plays a major role.

Figure 15 (next page) shows a plot of the measured peak intensity of the long-wavelength spectral component as a function of the sample temperature. The signal peaks near T = 35K where the P-line dominates the spectrum, and decreases roughly exponentially with increasing temperature. The emission persists to room temperature. The inset in Figure 3 is an Arrhenius plot of the same data. An excellent fit to the exponential high temperature falloff can be made, indicating that

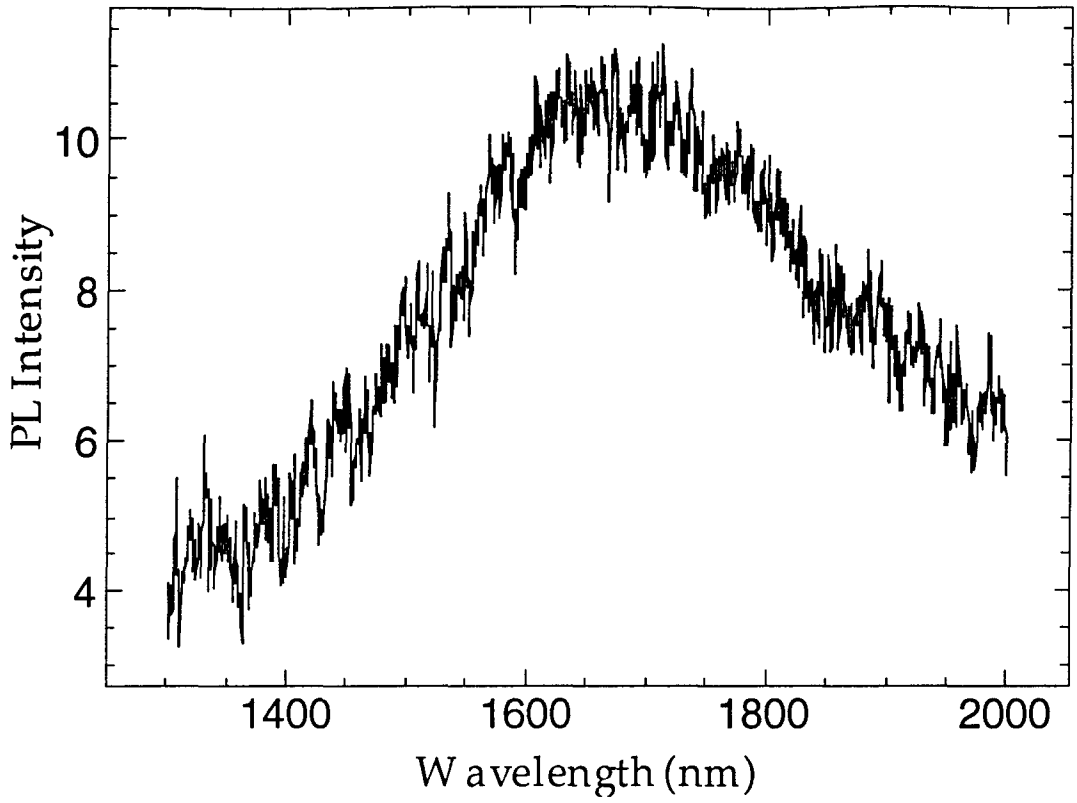

Figure 14. Room-temperature spectrum using an InAs detector.

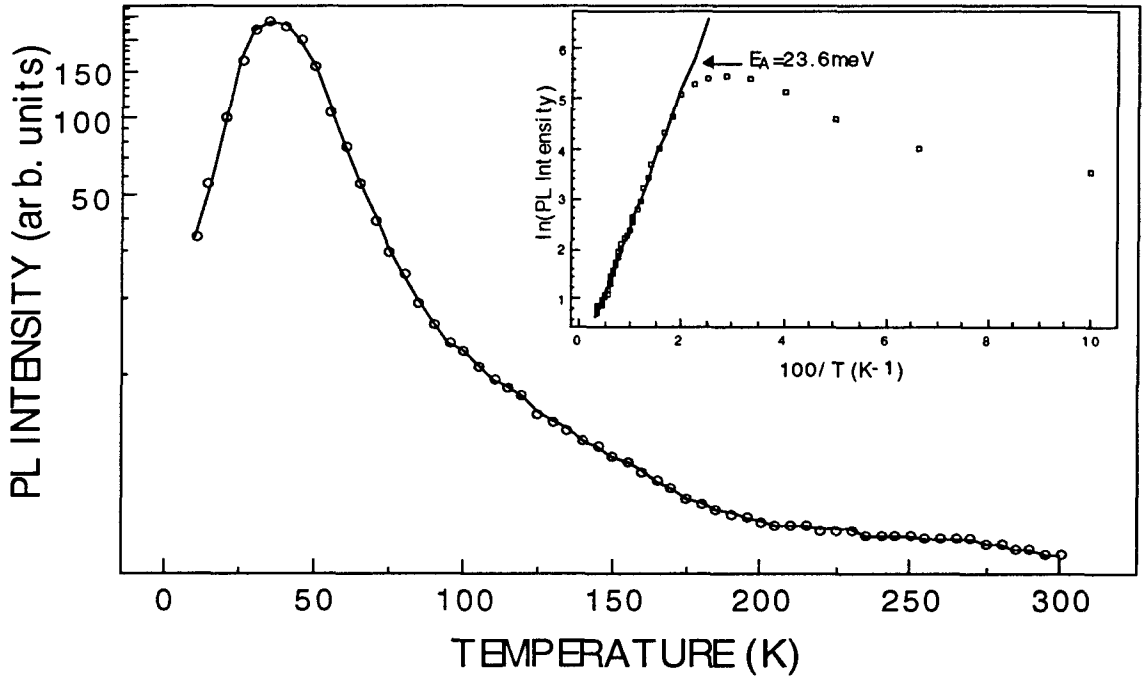

Figure 15. Measured temperature dependence.

the luminescence is quenched by a thermally activated process where E_A = 23.6 meV. It deserves mention that there is an earlier brief report of a similar luminescent system produced in silicon annealed under similar conditions to those used in this work [7]. Those authors reported spectra similar to those in Figure 13 (using a Ge detector), and a similar enhancement of the band-edge luminescence. However, they also noted that the luminescence peaks in strength at T = 280K and can be observed at temperatures up to T = 600K. Such a temperature dependence is clearly at odds with our own measurements. The behavior shown in Figure 15 is typical of a large number of samples examined in our laboratory. It is possible that the emission in Reference [7] arises from a different mechanism than the one at work in our samples, but it is difficult to say that with certainty.

We have measured the external quantum efficiency η of the sample used to obtain the spectra in Figures 13 and 14. The measurement was made by first determining the spectral responsivity of our detection system using a calibrated blackbody source at T = 1000°C. This enabled us to measure the external spectral quantum efficiency of the sample, which was then integrated over the wavelength extent of a given spectral feature to yield the total external quantum efficiency of the sample. At T = 77K, we obtained for the long-wavelength component of the spectrum $\eta \sim 5 \times 10^{-5}$, and for the enhanced band-edge luminescence, $\eta \sim 3 \times 10^{-5}$. At T = 300K, the peak intensity of the long-wavelength component is less than at T = 77K, but the feature is also broader, resulting in only a small drop in the external efficiency to $\eta \sim 2.5 \times 10^{-5}$. It is interesting that the efficiency of the emission reported here is actually comparable, at room temperature, to the efficiency reported for more complex structures, such as silicon-germanium/silicon quantum wells. We suspect that the emission described here results from a relatively small concentration of impurity complexes, so there might well be an opportunity to increase the efficiency if the nature of the complex can be determined.

We have found that for every Si sample investigated to date, the appearance of the P-line signal at T = 35K is always accompanied by the long-wavelength (near λ = 1.7 μm) spectral component at room temperature. We have also observed that both of these luminescence features disappear if the sample is heated above 600°C. The formation kinetics of the P-line defect have been carefully studied [8], with particular attention paid to the similarity to the formation of thermal donors in samples heated to T = 450°C. Early studies led to conjectures that thermal donors might be responsible for the low-temperature P-line emission. This was later shown not to be the case based on spectroscopic arguments [9].

Figure 16 shows the results of an isothermal annealing study in which we have measured the relative peak PL intensities of the long-wavelength luminescence component for T = 35K and T = 300K as a function of anneal time at 450°C. For comparison, we also measured the change in conductivity, approximately proportional to the number of thermal donors formed during the anneal. For this study, eleven samples were taken from a single commercially prepared, CZ-grown, 40 Ω-cm, p-type, <100> oriented wafer and annealed for various times. A small piece was taken from each sample for the PL

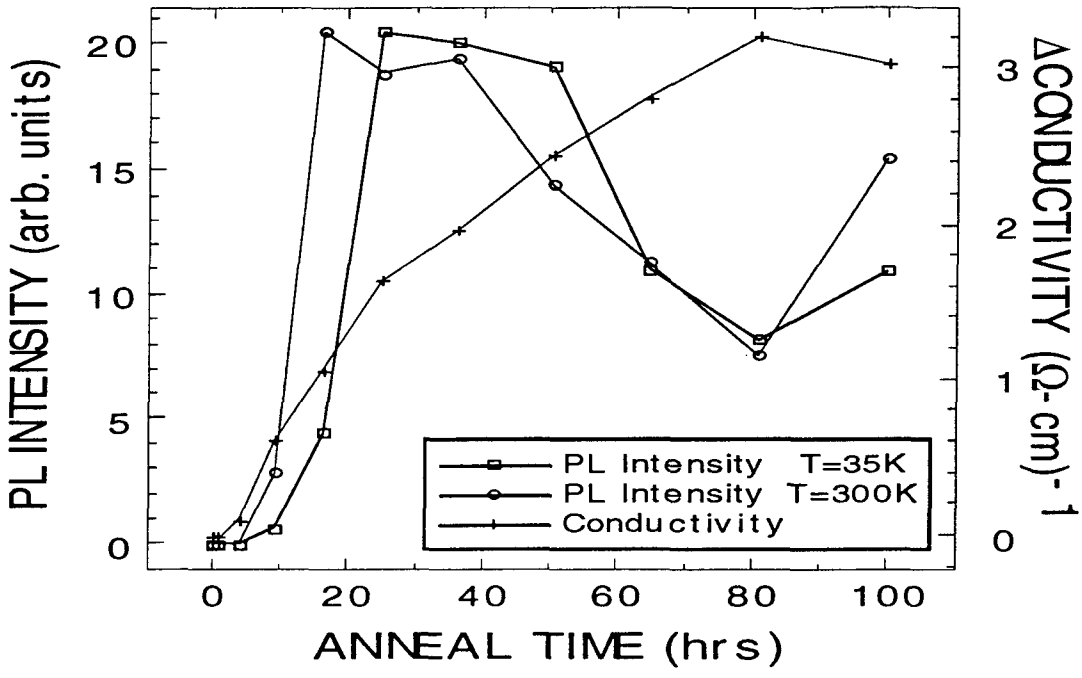

Figure 16. Measured annealing behavior.

measurements at both temperatures. In order to ensure that an accurate comparison could be made between the low- and room- temperature annealing curves, care was taken not to disturb the samples between measurements. In this way, sample-dependent and optical-alignment measurement errors were reduced to a minimum. The remainder of the sample was used to monitor the change in conductivity as measured at room temperature by a standard four-point probe technique. It is clear from the data that the luminescent centers evolve more rapidly than does the total thermal donor population. It also appears that the P-line at T = 35K develops slightly more quickly than does the broad, room-temperature feature near $\lambda = 1.7$ μm.

The fact that these two features form in the same samples (which must be oxygen rich) under similar thermal conditions leads us to believe that the defects responsible must be closely related. A spectroscopic study of the P-line luminescence in CZ-grown silicon isotopically enriched with ^{13}C and ^{18}O has led to a structural model of the defect which includes an interstitial carbon atom bound to a di-oxygen molecule or a related oxygen aggregate [10]. It may be the case that the different bands arise from two metastable configurations of the same defect constituents.

That the conductivity rises steadily in Figure 16 indicates that thermal-donor complexes are forming continuously during our 450°C anneal. IR-absorption-spectroscopy experiments used to characterize the formation of 450°C thermal donors have shown that the thermal donor population consists of a family of at least eleven distinguishable defects having slightly different binding energies. The situation is admittedly complicated. More work will be required to identify

unambiguously the origin of the room-temperature emission near wavelength λ = 1.7 μm. But it encouraging to have an example of room-temperature near-infrared emission from silicon.

VIII. Calculated Threshold for a Si-Based Laser

Because there are are as yet no reported demonstrations of a Si-based laser under any conditions, it is inviting to consider the possibility of doing so using the Be-related radiative isoelectronic bound exciton in silicon. If this can be done under any circumstances, no demonstration could invigorate the semiconductor community more.

We have explored this question theoretically by calculating the lasing threshold for a hypothetical Si:Be laser. In order to do this in a sensible way, we had to select a geometry that holds promise. We chose to introduce the Be impurities into a silicon-on-insulator (SOI) optical waveguide, the structure for which is illustrated below in Fig. 17. As we have demonstrated, high-quality SOI waveguides

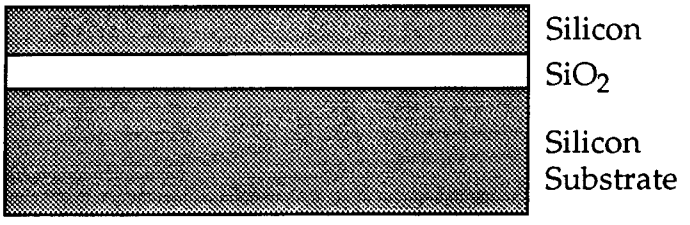

Figure 17. Silicon-on-insulator optical waveguide.

can be fabricated using the bond-and-etchback process. We have also demonstrated that radiative Be complexes can readily be formed in the thin silicon waveguide layer (upper layer in Fig. 17) in the SOI system.

Using a theoretical framework I developed several years ago [11,12], one that takes into account the size, shape, and location of the laser-mode's electric-field distribution (in this case, the waveguide mode) and the spatial distribution of the gain (in this case, the distribution of the Be impurities), graduate student Karen Moore carried out a series of model calculations to determine the lasing threshold for an SOI Si:Be system. The waveguide parameters were taken to be as follows, corresponding to layer thicknesses for SOI wafers we have in hand: SiO_2 thickness of 1.0 micron, Si-layer thickness of 1.39 microns. A few results from the calculation appear in Figure 18 (see next page), where the threshold, here represented as the minimum Be density required to achieve threshold, is plotted as a function of the cavity length of the laser. Naturally, the threshold condition depends on the reflectivity of the laser, so results are shown for three cases, reflectivities of R = 31%, 60%, and 90%. These results are very encouraging. They show that for cavity lengths of only a few mm and only modestly high cavity reflectivities, the lasing threshold can be reached with Be densities well below 10^{18} cm^{-3}. We are currently examining ways to test this prediction. We already have the SOI material,

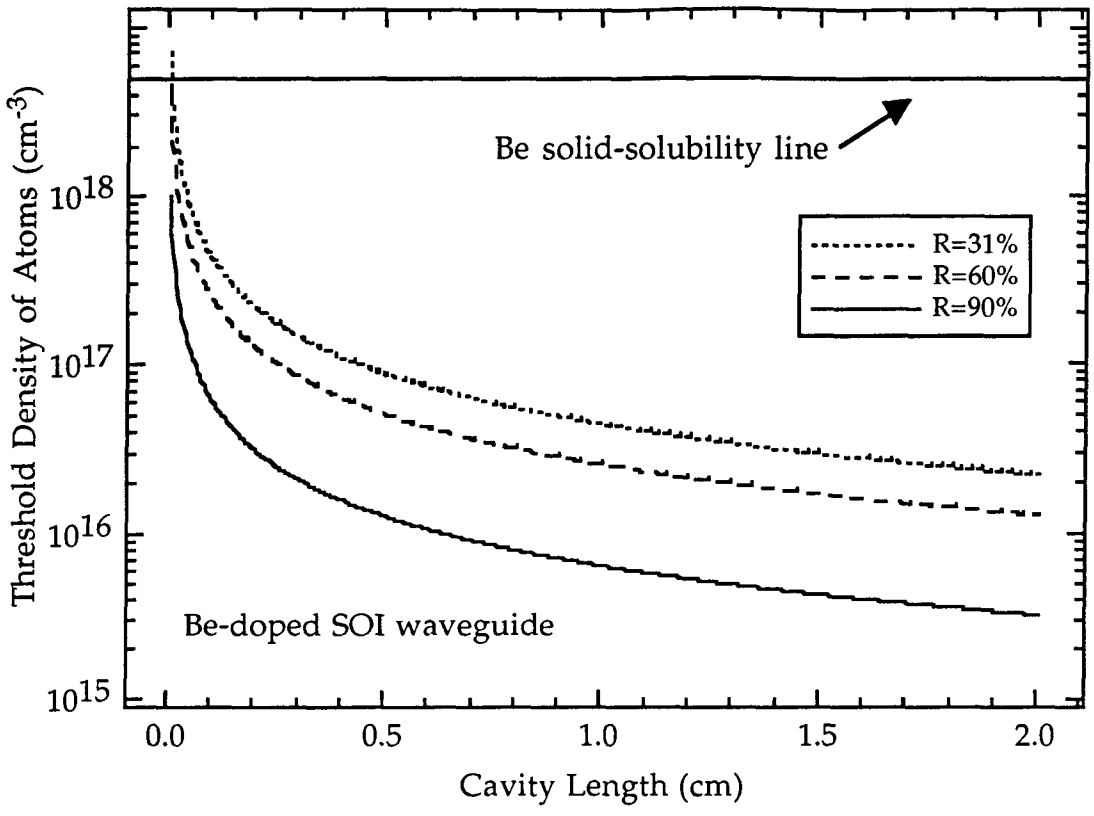

Figure 18. Calculated lasing threshold density vs. cavity length for the SOI Si:Be bound-exciton system.

and can certainly introduce the Be by implantation. The largest technical challenge for the experiment will be to fabricate good-quality cavity mirrors. For the orientation for which SOI material is available, Si does not cleave to give vertical facets, so we're exploring various etching and polishing options. Unfortunately, the funding period for this grant came to an end before a serious experimental attempt could be made to fabricate a structure in which lasing might be demonstrated.

Erbium-doped silicon has also been proposed as a possible mechanism for achieving lasing in Si. [13] For comparison, Karen Moore calculated the lasing thresholds for the SOI Si:Er system, and a few results appear in Figure 19 (see next page). Again, for sufficiently high mirror reflectivities, the lasing threshold is predicted to be achievable for Er densities below the solid-solubility limit, although the densities for Er are somewhat higher than those for Be.

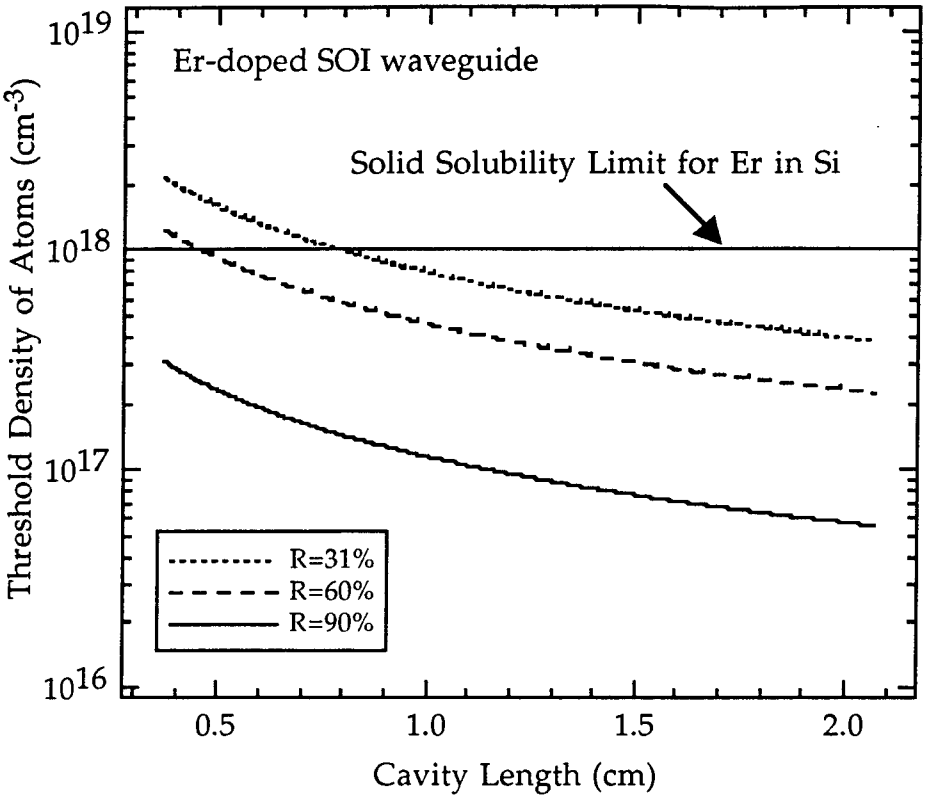

Figure 19. Calculated lasing threshold density vs. cavity length for the SOI Si:Er system.

IX. Additional Collaborations

As is often the case, new opportunities for collaboration presented themselves during the course of the research. Specifically, a collaboration with Prof. Irving Herman of the Applied Physics Department at Columbia University offered the opportunity to investigate some of the microscopic issues associated with the Be-related impurity complex in Si, SiGe alloys, and SiGe/Si superlattices. Prof. Herman and his students performed low-temperature photoluminescence measurements as a function of pressure (diamond anvil cell).

A collaboration with Prof. Philippe Fauchet of the Department of Electrical Engineering at the University of Rochester explored the photo- and electroluminescence properties of Si-rich silicon oxide (SRSO) layers. That work culminated in the recently reported demonstration of a room-temperature light-emitting diode that employed erbium-doped SRSO. [14] At room temperature, the LED produced emission near wavelength $\lambda = 1.5\ \mu m$, but with an efficiency ($\sim 1 \times 10^{-6}$) too low to be of practical importance.

X. Concluding Remarks

This program of research investigated the characteristics of radiative impurity complexes in Si, SiGe alloys, and SiGe/Si superlattices. The Be-related isoelectronic bound-exciton complex (pairs of Be atoms) that forms in Si was used as a prototype impurity complex to investigate quantum confinement effects in SiGe/Si superlattices. In order to demonstrate that confinement, it was necessary to develop a technique for introducing Be during MBE growth in such a way that Be pairs were formed. Once this was accomplished, quantum confinement of the associated bound exciton was demonstrated for several alloy compositions and quantum-well thicknesses. While some improvement in the temperature stability of the bound exciton was observed, the improvement was not large for the range of (Si-rich) alloy compositions examined so far. Further investigation will be required to determine the ultimate degree of improvement that can be achieved by quantum confinement. The idea of using quantum-confined bound-excitons to achieve efficient room-temperature optical emission from a silicon-based materials system remains an appealing one. Calculations indicate that Si:Be lasing should be possible in a suitably fabricated optical waveguide structure.

Room temperature optical emission was observed from an oxygen-related impurity complex in crystalline silicon. The photoluminescence spectrum peaked near wavelength $\lambda = 1.7\ \mu m$ with external efficiency at $T = 300$ K estimated to be approximately 2.5×10^{-5}. It is encouraging to find room-temperature luminescence in the near-infrared, but the efficiency of this particular impurity mechanism is too low at this point to be of practical use.

XI. References

1. Dennis G. Hall, "The role of silicon in optoelectronics," Mat. Res. Soc. Symp. Proc. Vol 298, 367 (1993).

2. R. A. Modavis, D. G. Hall, J. Bevk, and B. S. Freer, L. C. Feldman, and B. E. Weir, Appl. Phys. Lett. 57, 954 (1990).

3. T. G. Brown, P. L. Bradfield, D. G. Hall, and R. A. Soref, Opt. Lett. 12, 753 (1987).

4. R. A. Modavis, D. G. Hall, J. Bevk, and B. S. Freer, Appl. Phys. Lett. 59, 1230 (1991).

5. T.G. Brown and D.G. Hall, "Optical Emission at 1.32 μm from Sulfur-Doped Crystalline Silicon," Appl. Phys. Lett. 49, 245 (1986).

6. T.G. Brown, P.L. Bradfield, and D.G. Hall, "Concentration Dependence of Optical Emission from Sulfur-Doped Crystalline Silicon," Appl. Phys. Lett. 51, 1585 (1987).

7. J. Weber and R. Sauer, Mat Res. Soc. Symp. Proc. 14, 165 (1983).

8. See W. Kurner, R. Sauer, A Dornen, and K. Thonke, Phys. Rev B 39, 13,327(1989) and the references therein.

9. A. Dornen, R. Sauer, and J. Weber, "Annealing and Stress Study of Oxygen-Related Thermally Induced Defect Luminescence in Silicon," in Proceedings of the Thirteenth International Conference on Defects in Semiconductors, edited by L. C. Kimerling and J. M. Parsey, Jr. (The Metallurgical Society of AIME, New York, 1985), pp. 653-660.

10. See Ref. 7.

11. D. G. Hall, R. J. Smith, and R. R. Rice, "Pump-size Effects in Nd:YAG Lasers," *Appl. Opt.* 19, 3041 (1980).

12. D. G. Hall, "Optimum-Mode-Size Criterion for Low-Gain Lasers," *Appl. Opt.* 20,1579 (1981).

13. See, for example, Y. H. Xie, E. A. Fitzgerald, and Y. J. Mii. J. Appl. Phys. 70, 3223 (1991).

14. L. Tsybeskov, K. L. Moore, K. D. Hirschman, S. P. Duttagupta, D. G. Hall, and P. M. Fauchet, "Room-Temperature Photoluminescence And Electroluminescence From Er-Doped Silicon-Rich Silicon Oxide," Appl. Phys. Lett. 70, 1790 (1997).

Appendix -- General Information

The Institute of Optics

Founded in 1929, The Institute of Optics is the premier program of higher education in Optics in the United States. An academic department with a faculty made up of physicists, materials scientists, and engineers, The Institute serves approximately 100 undergraduate majors pursuing the B.S. degree in Optics and 100 graduate students, 75 of whom are pursuing the Ph.D. in Optics. In the 1995 National Research Council ranking of doctoral programs, The Institute of Optics was included in the survey for the first time in history and placed in the Physics category. The Institute ranked 25th out of 147 Physics programs in the overall ranking, an outstanding performance for a department centered on a narow range of subfields. Even more impressive, The Institute of Optics ranked first out of 147 departments in publications per faculty member during the survey period (1988 - 1992), second out of 147 in percentage of faculty with external research support, 11th out of 147 in faculty effectiveness, and 15th out of 147 in citations per faculty member in the survey period. Ph.D. graduates of The Institute of Optics can be found on such research-oriented Physics faculties as those of Duke, Penn State, Lehigh, Cornell, and Sydney Universities; on the teaching-oriented faculties of such small schools as Christian Brothers University (Tennessee), Mt. Vernon Nazarene College (Ohio), and Reed College (Oregon), among others; and in the employ of federal laboratories, small and medium size companies, and such major corporations as AT&T, Lucent, IBM, Xerox, and Eastman Kodak.

The Institute of Optics Home Page http://www.optics.rochester.edu/

Dennis G. Hall is William F. May Professor and Director of The Institute of Optics at the University of Rochester. He is a Fellow of the Optical Society of America (OSA), the American Physical Society (APS), and the International Society for Optical Engineering (SPIE), is a former (elected) member of the OSA Board of Directors, and is a Topical Editor of the Journal of the Optical Society of America. Prof. Hall is the recipient of two undergraduate teaching awards, the author of more than 120 refereed journal articles and several book chapters, and the editor of the 1993 reprint volume *Coupled-Mode Theory in Guided-Wave Optics* (SPIE Press). He has supervised to completion fourteen Ph.D. theses and six M.S. theses.

Karen L. Moore Sullivan is a doctoral candidate in The Institute of Optics at the University of Rochester. She earned the B.S. degree (with High Distrinction) in Optics at the University of Rochester in 1990, and the M.S. degree in Optics from the University of Rochester in 1991. She entered the doctoral program in Optics in September 1991, and plans to graduate during 1997. She is an active member of the Materials Research Society and the author of seven refereed publications. Her doctoral thesis research on radiative impurity complexes in Group IV semiconductors was supported to a large degree by the Air Force Office of Scientific Research.